

MEASURING SURFACE SUBSIDENCE IN WUHAN, CHINA WITH SENTINEL-1 DATA USING PSINSAR

Benattou, Mustapha Mehdi^{1,*}, Balz, Timo¹, Liao, Minsheng¹

¹ State Key Laboratory of Information Engineering in Surveying, Mapping and Remote Sensing (LIESMARS), Wuhan 43007, China – (benattou.mehdi@yahoo.com)

KEY WORDS: Subsidence Monitoring, TOPS, PSInSAR, Hazards, Sentinel, SARPROZ

ABSTRACT:

We use the potential of Sentinel-1 for urban subsidence monitoring. A case study was conducted in Wuhan using Sentinel-1A images acquired from 22nd June 2015 to the 24th of April 2017 acquired from an ascending orbit. Our results using PSInSAR are compared to a recent study using SBAS. Moreover, in another experiment, only more recent data, containing 18 images from the 7th of March 2017 to the 14th of March 2018, have been processed in order to analysis changes in the subsidence behavior over the study area. In addition to that, the proposed method (PSInSAR) was used to measure the water height in the east lake using metallic objects as stable PS points.

1. INTRODUCTION

Surface subsidence is one of the most common geotechnical hazards and widespread in cities, which may result from human activities such as underground construction or/and groundwater extraction or non-human-activities (e.g., earthquake, faults)(Bai et al., 2016). it is often caused by consolidation and compression of underground unconsolidated strata (Zhou et al., 2017). Surface subsidence is also one of the major disasters that can cause serious damage to infrastructures, tunnels, roads, bridges, and buildings, which made a huge impact to the safety of the cities (Guo et al., 2017; Zhou et al., 2017).

With its long history of subsidence, way back to the 1930s (Fan, 2006), Wuhan still continuously suffers from this hazards due to the fast urban development and subway constructions (Goethals, 2011). Compared to single-point-measurement methods such as ground leveling (Baldi et al., 2009; Poland et al., 2006) or Global Navigation Satellite System (GNSS) (Carminati et al., 2002; Psimoulis et al., 2007), Differential Interferometric Synthetic Aperture Radar (D-InSAR) has been developed to measure relatively slow surface motion between two SAR image acquisitions (Avallone et al., 1999) and it has been used widely for subsidence monitoring (Cigna et al., 2012; Solari et al., 2016). This technique allows monitoring large areas at comparably low cost with accuracy within centimeters to millimeters (Tosi et al., 2016). However, this technique has limitations (Bürgmann et al., 2000), amongst are the temporal decorrelation, geometrical decorrelation, and the variations in atmospheric conditions which might reduce the monitoring accuracy. In order to overcome the main limitations of this technique, PSInSAR has been developed to measure surface motion and analyze the temporal Earth surface displacement (Ferretti et al., 2001) based on the so-called Permanent Scatterers (Psimoulis et al., 2007) where interferograms are formed using a single master scene and analyzed at single look resolution (Agram, 2010).

The Sentinel 1A/B constellation offers a global coverage. The data is provided free of charge by the European Space Agency (ESA). Large areas can be studied, because Sentinel-1 is using TOPS (Terrain Observation by Progressive Scans) mode with

5m×20m (range × azimuth) spatial resolution and around 250km swath width.

Many studies have been realized in this area using different methods as well as different sources of data (Bai et al., 2016; Costantini et al., 2016; Guo et al., 2017), in the following sections we are going to show the data used, the methodology and the results obtained using the proposed technique.

2. STUDY AREA AND DATASET

Wuhan is the capital of Hubei province, it is located in central China in the east of Jiangnan Plain and southern slope of Tappieh mountains with geographical coordinates of 114° 17' 0" E, 30° 35' 0" N. Wuhan is a rather new conglomerate of historically three independent cities: Wuchang, Hankou, and Hanyang. The city has many lakes and is on the intersection of the Yangtze river and the Han river, which from 25 percent of Wuhan's total surface (Hendrischke, 2013).

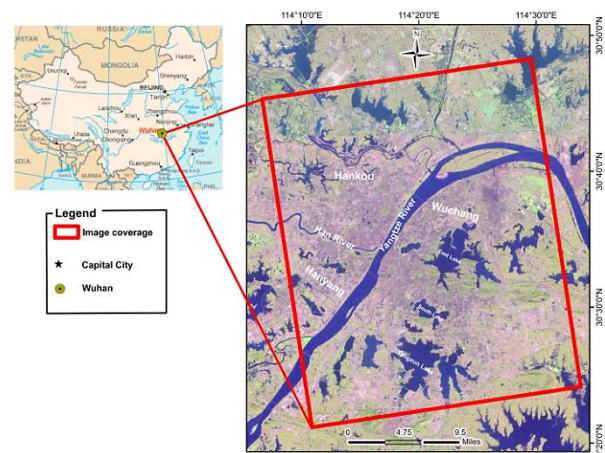


Figure 1. Location of the Sentinel study area displayed on Sentinel 2 image acquired on the 11th October 2017.

* Corresponding author

Terrain Observation by Progressive Scans mode (TOPS) Interferometric wide (IW) with $5\text{ m} \times 20\text{ m}$ (range \times azimuth) spatial resolution and around 250 km coverage have been chosen due to its wide coverage and its short revisit time which is 12 days for sentinel 1A/B separately and 6 days if we combine both systems.

The Sentinel1 data used in this paper is provided by the European Space Agency. The following table shows the parameters of interferometric wide (IW) TOPS acquisition mode. Additionally, we used the SRTM DEM.

Sentinel-1A/B	
Parameters	Interferometric Wide Swath (IW3)
Incidence angle	43.9°
Resolution (range and azimuth)	5 m \times 20 m
Operating band	C (5.547 cm)
Ground swath width	250 km
Orbit	Ascending
Polarization	VV

Table1: Sentine-1A parameters and its twin Sentinel-1B for Interferometric Wide Swath used in the processing

3. METHODOLOGY AND RESULTS

The data have been divided into two stacks or temporal intervals to allow us to study the subsidence in details; the first stack includes 36 sentinel1A images acquired from the 22nd of June 2015 to the 24th of April 2017 in order to compare it with the results found in the proposed paper using SBAS approach by (Zhou et al., 2017), the second stack include 18 images acquired from the 7th of March 2017 till the 14th of March 2018 to follow the subsidence till recent dates using the sentinel1 continuously due to the constant global coverage .

The following figure shows the vertical deformation map of the 36 images with master image dated on the 12th of March 2016 processed by SARPROZ (www.sarproz.com).

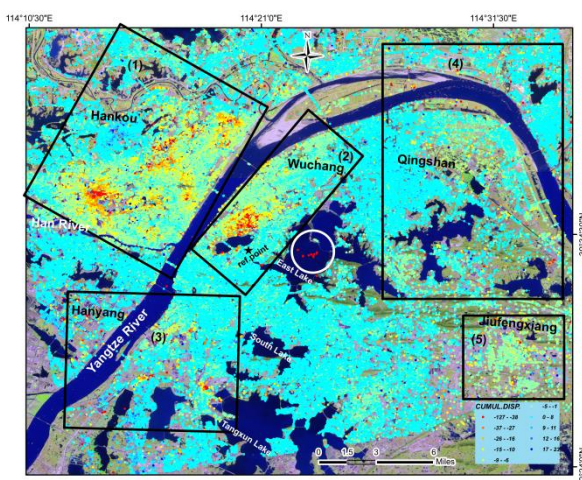


Figure 2: Line of Sight deformation by PSInSAR displayed on Sentinel 2 image acquired on the 11th October 2017

The line of sight (LOS) deformation map shows five subsidence areas distributed all over Wuhan, with an average deformation ranging from -12.7 cm/year to 2.3 cm/year. However, Zhou et al (2017) used different interferometric SAR method (SBAS) and

found only four subsidence areas with an average deformation ranging from -8.2 cm/year to 1.8 cm/year. In addition to that, we found a new subsidence area in the southeast of the city named (5) (figure.2);

The second stack we processed contains 18 images acquired between the 7th of March 2017 and the 14th of March 2018. We processed with a single master image (23rd of June 2017).

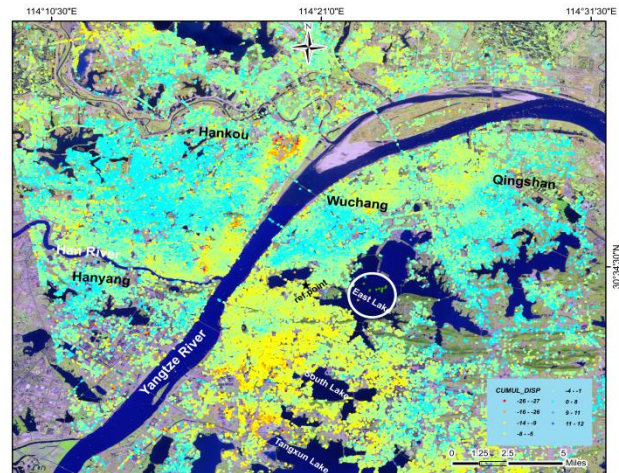


Figure 3. Line of Sight deformation by PSInSAR displayed on Sentinel 2 image acquired on the 11th October 2017

The figure above shows the cumulative displacement in the line of sight (LOS). Generally, the information extracted from the map indicates a deformation ranging from -2.7 cm/year to 1.2 cm/year. This shows the general reduction of the estimated deformation in the area of Hankou with an increasing of the surface subsidence in Wuchang area.

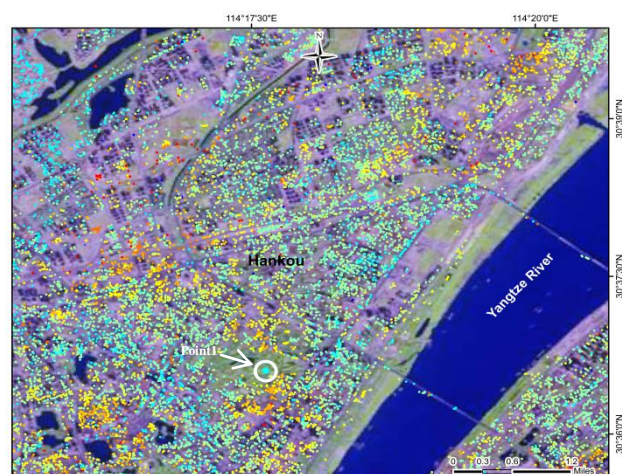


Figure4.Zoomed image from the first stack in Hankou area

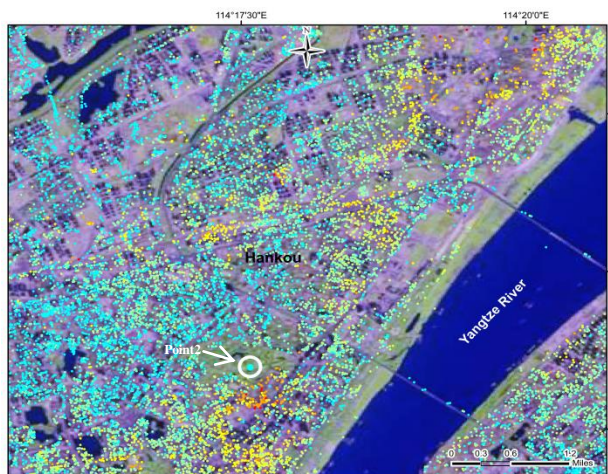


Figure 5. Zoomed image from the second stack in Hankou area

The following two graphs represent the deformation time series of the selected point (point1, point2)¹ from figure 5, figure 6 successively.

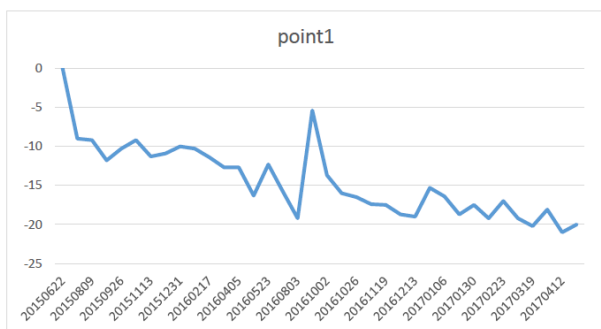


Figure 6. Time series of point1 from the first stack (figure.4)

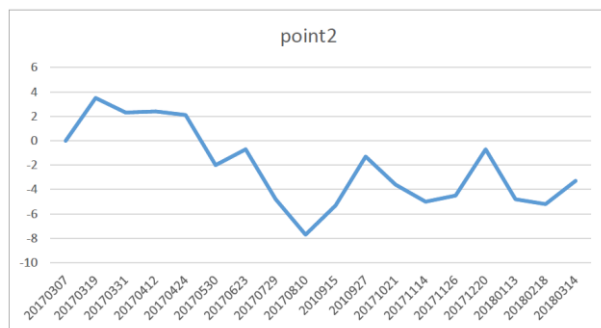


Figure 7. Time series of point2 from the second stack (figure.5)

A second point (point3, point4)² was selected in Wuchang area to see time series deformation changes in the two stacks (first stack, second stack)



Figure 8. Zoomed image from the first stack in Wuchang area



Figure 9. Zoomed image from the second stack in Wuchang area

Figure 10, figure 11 represent the time series deformation of point3 (figure 8), point4 (figure 9) successively;

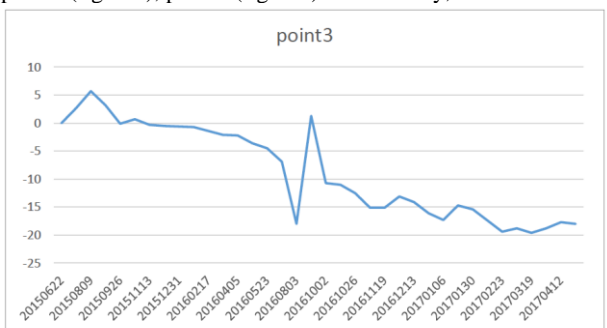


Figure 10. Time series of point1 from the first stack (figure.8)

¹ Point1, point2 are the same.

² Point3, point4 are the same.

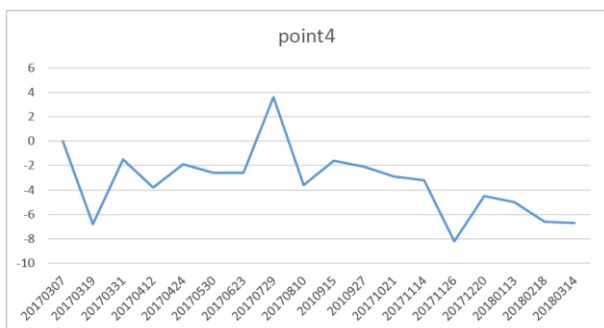


Figure 11. Time series of point1 from the first stack (figure.9)

SAR is not responsive to water, which means, we generally expect no PS points on water surfaces. However, we found a couple of stable points on Wuhan's East Lake in the final result,

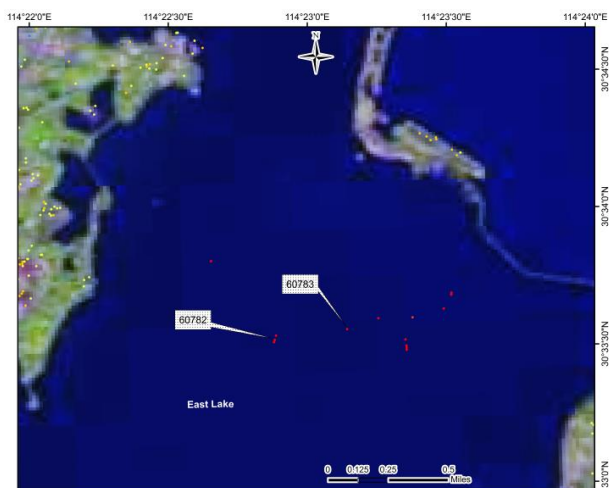


Figure 12. Stable PS points detected in the East Lake (donghu)

After confirming the relative interferometric stability of these points, we felt the need to analyze the situation in situ. As it turns out, there are series of metallic poles to be found spread over the East Lake.



Figure 13. Metallic pillars located in the East Lake

We can take advantage from these PS points located in the East Lake to measure the water height (water level), Two PS points named successively 60782, 60783 (Figure 13) were chosen to see if their movement is correlated or not as it is shown in figure14.

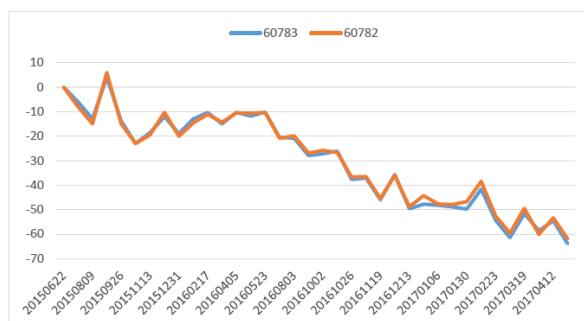


Figure 14. Points 60783, 60783 deformation trend from 22/06/2015 until 24/04/2017

Figure 14 shows that Points 60782 and 60783 are following the same deformation trend,

4. CONCLUSION

East Lake is one of the most important water bodies in Wuhan city; it needs a periodic observation to know the water height changes, in this case PSInSAR can be used to measure the water level in the East Lake by considering the metallic pillars planted in the lake as a stable PS points.

ACKNOWLEDGMENTS

The work presented here was supported by the Natural Science Foundation of China under Grant No.61331016. The data has been processed using SarProZ developed by Dr. Daniele Perissin.

REFERENCES

- Agram, P. S. (2010). Persistent scatterer interferometry in natural terrain. stanford university.
- Avallone, A., Zollo, A., Briole, P., Delacourt, C., & Beauducel, F. (1999). Subsidence of Campi Flegrei (Italy) detected by SAR interferometry. *Geophysical Research Letters*, 26(15), 2303-2306.
- Bai, L., Jiang, L., Wang, H., & Sun, Q. (2016). Spatiotemporal characterization of land subsidence and uplift (2009–2010) over wuhan in central china revealed by terrasar-X insar analysis. *Remote Sensing*, 8(4), 350.
- Baldi, P., Casula, G., Cenni, N., Loddo, F., & Pesci, A. (2009). GPS-based monitoring of land subsidence in the Po Plain (Northern Italy). *Earth and Planetary Science Letters*, 288(1-2), 204-212.
- Bürgmann, R., Rosen, P. A., & Fielding, E. J. (2000). Synthetic aperture radar interferometry to measure Earth's surface topography and its deformation. *Annual review of earth and planetary sciences*, 28(1), 169-209.

- Carminati, E., & Martinelli, G. (2002). Subsidence rates in the Po Plain, northern Italy: the relative impact of natural and anthropogenic causation. *Engineering Geology*, 66(3-4), 241-255.
- Cigna, F., Osmanoglu, B., Cabral-Cano, E., Dixon, T. H., Ávila-Olivera, J. A., Garduño-Monroy, V. H., . . . Wdowinski, S. (2012). Monitoring land subsidence and its induced geological hazard with Synthetic Aperture Radar Interferometry: A case study in Morelia, Mexico. *Remote Sensing of Environment*, 117, 146-161.
- Costantini, M., Bai, J., Malvarosa, F., Minati, F., Vecchioli, F., Wang, R., . . . Li, J. (2016). Ground deformations and building stability monitoring by COSMO-SkyMed PSP SAR interferometry: Results and validation with field measurements and surveys. Paper presented at the Geoscience and Remote Sensing Symposium (IGARSS), 2016 IEEE International.
- européenne, A. s. (2012). Sentinel-1: ESA's Radar Observatory Mission for GMES Operational Services: ESA communications production.
- Fan, S. (2006). A discussion on karst collapse in Wuhan (Hubei). *Resour. Environ. Eng*, 20, 608-616.
- Ferretti, A., Prati, C., & Rocca, F. (2001). Permanent scatterers in SAR interferometry. *IEEE Transactions on geoscience and remote sensing*, 39(1), 8-20.
- Goethals, S. (2011). The influence of interactions between urban and transportation planning through the transforming structures of Chinese big cities. How to integrate current decentralized concentration and urban mobility management. Paper presented at the 47th ISOCARP Congress, October.
- Guo, J., Hu, J., Li, B., Zhou, L., & Wang, W. (2017). Land subsidence in Tianjin for 2015 to 2016 revealed by the analysis of Sentinel-1A with SBAS-InSAR. *Journal of Applied Remote Sensing*, 11(2), 026024.
- Hendrichske, H. (2013). *The Political Economy of China's Provinces: Competitive and Comparative Advantage*: Routledge.
- Poland, M., Bürgmann, R., Dzurisin, D., Lisowski, M., Masterlark, T., Owen, S., & Fink, J. (2006). Constraints on the mechanism of long-term, steady subsidence at Medicine Lake volcano, northern California, from GPS, leveling, and InSAR. *Journal of Volcanology and Geothermal Research*, 150(1-3), 55-78.
- Psimoulis, P., Ghilardi, M., Fouache, E., & Stiros, S. (2007). Subsidence and evolution of the Thessaloniki plain, Greece, based on historical leveling and GPS data. *Engineering Geology*, 90(1-2), 55-70.
- Solari, L., Ciampalini, A., Raspini, F., Bianchini, S., & Moretti, S. (2016). PSInSAR analysis in the Pisa Urban Area (Italy): A case study of subsidence related to stratigraphical factors and urbanization. *Remote Sensing*, 8(2), 120.
- Tosi, L., Da Lio, C., Strozzi, T., & Teatini, P. (2016). Combining L-and X-band SAR interferometry to assess ground displacements in heterogeneous coastal environments: the Po River Delta and Venice Lagoon, Italy. *Remote Sensing*, 8(4), 308.
- Zhou, L., Guo, J., Hu, J., Li, J., Xu, Y., Pan, Y., & Shi, M. (2017). Wuhan Surface Subsidence Analysis in 2015–2016 Based on Sentinel-1A Data by SBAS-InSAR. *Remote Sensing*, 9(10), 982.